Hydrogen Bonding and Structural Motifs in Organic L-Malate(2−) Salts

Christer B. Aakeröy and Mark Nieuwenhuyzen

School of Chemistry, The Queen's University of Belfast, Belfast BT9 5AG, Northern Ireland

Received November 2, 1995. Revised Manuscript Received March 28, 1996[⊗]

To examine packing preferences and hydrogen-bond patterns in organic L-malate salts $[AH_2][mal]$ or $[AH]_2[mal]$ (where A = amine), the syntheses and crystal structures of six new salts, bis(4-chlorobenzyl)ammonium(1+) L-malate(2−) monohydrate (**1**), ethylenediammonium(2+) L-malate(2−) (**2**), piperazinium(2+) L-malate(2−) monohydrate (**3**), bis(3-methylbenzyl)ammonium(1+) L-malate(2−) (**4**), bis(3-chlorobenzyl)ammonium(1+) L-malate(2−) monohydrate (**5**), and 1,6-hexanediammonium(2+) L-malate monohydrate (**6**), are presented. In contrast to the structurally consistent hydrogen malate salts, these compounds show a variety of unpredictable packing patterns which demonstrates that the removal of a single hydrogen-bond interaction can substantially alter the structure of a family of ionic compounds. This observation lends considerable support to design strategies which employ hydrogen bonding as means of linking ionic building blocks into predictable multidimensional architectures. The structural effects of hydrogen bonding is discussed in detail, and the use of a combination of single-crystal and powder X-ray diffraction techniques for assessing structural purity is addressed.

Introduction

The ability to design new materials with predictable structures and properties remains an elusive, albeit highly desirable, goal, and despite considerable efforts, the development of "the phase of crystal engineering"[1] remains incomplete. The key obstacle is the problem of controlling the positional and orientational freedom of molecular building blocks,[2] and much work has focused on the intentional design of 1-D (chains, ribbons, tapes) and 2-D (sheets and layers) motifs in order to reduce the spatial freedom of individual units, notably in molecular solids.[3] The hydrogen bond is now emerging as a powerful tool in the design of new organic salts, and it has been shown that hydrogentartrate anions can be used as building blocks of reliable 2-D anionic layers.[4,5] For example, the synthesis and characterization of a material with useful nonlinear optical properties, imidazolium hydrogen tartrate, were first reported in 1993.[6] The same structure (and an outline of this strategy) was recently presented again by Carlin and co-workers, although the original paper was not cited.[7]

To further the area of crystal engineering, we need to improve our understanding of the structural effects that individual hydrogen bonds exert on the resulting 3-D solid. In addition, new building blocks of multidimensional architectures need to be identified and tested, in order to provide both flexibility to synthetic programs and new model systems for theoretical examinations.

Recently, malic acid has received attention in this context as a source of building blocks (the hydrogen malate anion) for crystal engineering. These anions have a propensity to form infinite 2-D layers, even in the presence of a variety of counterions,[8] and the basis for this reoccurring motif is provided by complimentary hydrogen-bonding sites; invariably, adjacent anions are linked into infinite chains through a head-to-tail O−H···O interaction. The α-hydroxyl group commonly produces a cross-link between neighboring chains, thereby generating an infinite layer. However, if the basis for this motif is removed (e.g., by deprotonating both ends of the dicarboxylic acid), how will this influence the occurrence of repeatable packing patterns in these salts? It was our contention[8] that the possibility of a head-to-tail hydrogen bond between neighboring anions was essential for the formation of these networks, and that, by removing this single hydrogen bond, the predictability of the resulting ionic aggregation in this family of compounds would be severely diminished. A search of the Cambridge Structural Database[9] for organic

[⊗] Abstract published in *Advance ACS Abstracts,* May 1, 1996.

(1) Schmidt, G. M. J. *Pure Appl. Chem.* **1971**, *27*, 647.

(2) (a) Desiraju, G. R. *Crystal Engineering: The Design of Organic Solids*; Elsevier: Amsterdam, 1989. (b) Mathias, J. P.; Stoddart, J. F. *Chem. Soc. Rev.* **1992**, *21*, 215. (c) Aakeröy, C. B.; Seddon, K. R. *Chem. Soc. Rev.* **1993**, *22*, 397. (d) Subramanian, S.; Zaworotko, M. *Coord. Chem. Rev.* **1994**, *137*, 357.

(3) Some examples of crystal engineering of molecular solids: (a) Seto, C. T.; Whitesides, G. M. *J. Am. Chem. Soc.* **1991**, *113*, 9025. (b) Zhao, X.; Chang, Y.-L.; Fowler, F. W.; Lauher, J. W. *J. Am. Chem. Soc.* **1990**, *112*, 6627. (c) Weber, E.; Finge, S.; Csöregh, I. *J. Org. Chem.* **1991**, *56*, 7281. (d) Lehn, J.-M.; Mascal, M.; DeCian, A.; Fischer, J. *J. Chem. Soc., Perkin Trans. 2* **1992**, 461. (e) Simard, M.; Su, D.; Wuest, J. D. *J. Am. Chem. Soc.* **1991**, *113*, 4696. (f) Garcia-Tellado, F.; Geib, S. J.; Goswami, S.; Hamilton, A. D. *J. Am. Chem. Soc.* **1991**, *113*, 9265. (g) Thalladai, V. R.; Panneerselvam, K.; Carrell, C. J.; Carell, H. J.; Desiraju, G. R. *J. Chem. Soc., Chem. Commun.* **1995**, 341. (h) Etter, M. C. *J. Phys. Chem.* **1991**, *95*, 4601.

(4) Aakeröy, C. B.; Hitchcock, P. B.; Seddon, K. R. *J. Chem. Soc., Chem. Commun.* **1992**, *553*.

(5) (a) Zyss, J.; Pecaut, J.; Levy, J. P.; Masse, R. *Acta Crystallogr.* **1993**, *B49*, 334. (b) Dastidar, P.; Row, T. N. G.; Prasad, B. R.; Subramanian, C. K.; Bhattacharya, S. *J. Chem. Soc., Perkin Trans. 2* **1993**, *12*, 2419. (c) Watanabe, O.; Noritake, T.; Hirose, Y.; Okada, A.; Kurauchi, T. *J. Mater. Chem.* **1993**, *23*, 321.

(6) Aakeröy, C. B.; Hitchcock, P. B. *J. Mater. Chem.* **1993**, *3*, 1129.

(7) Fuller, J.; Carlin, R. T.; Simpson, L. J.; Furtak, T. E. *Chem. Mater.* **1995**, *7*, 909.

(8) (a) Aakeröy, C. B.; Nieuwenhuyzen, M. *J. Am. Chem. Soc.* **1994**, *116*, 10983. (b) Aakeröy, C. B.; Nieuwenhuyzen, M. *J. Mol. Struct.* **1996**, *347*, 223.

(9) Cambridge Crystallographic Database, version 5.09 (April 1995). Allen, F. H.; Kennard, O.; Taylor, R. *Acc. Chem. Res.*, **1983**, *16*, 46.

S0897-4756(95)00524-2 CCC: $12.00

Table 1. Data Collection and Refinement for 1−6

crystal data	**1**	**2**	**3**	**4**	**5**	**6**
empirical formula	$C_{18}H_{24}Cl_2N_2O_6$	$C_6H_{14}N_2O_5$	$C_8H_{18}N_2O_5$	$C_{20}H_{28}N_2O_5$	$C_{18}H_{24}N_2O_6$	$C_{10}H_{24}N_2O_6$
MW	433.29	194.19	238.24	376.44	435.29	268.31
crystal size (mm)	0.76 × 0.35 × 0.05	0.73 × 0.51 × 0.18	0.64 × 0.54 × 0.32	0.61 × 0.36 × 0.33	0.88 × 0.18 × 0.16	0.33 × 0.32 × 0.11
crystal system	triclinic	orthorhombic	orthorhombic	monoclinic	monoclinic	triclinic
space group	*P*1 (No. 1)	$P2_12_12_1$ (No. 19)	$P2_12_12_1$ (No. 19)	$P2_1$ (No. 4)	$P2_1$ (No. 4)	*P*1 (no. 1)
a (Å)	4.835(1)	5.980(1)	6.711(1)	10.011(2)	4.846(1)	8.786(1)
b (Å)	5.744(1)	8.569(1)	10.437(1)	8.381(2)	35.267(6)	9.679(1)
c (Å)	17.676(3)	17.877(1)	15.577(2)	12.779(4)	5.753(1)	9.911(1)
α (deg)	96.13(3)	90	90	90	90	62.15(1)
β (deg)	96.62(4)	90	90	107.27(2)	95.69(2)	78.90(1)
γ (deg)	95.42(5)	90	90	90	90	67.10(1)
volume (Å^3)	458.1(2)	916.1(2)	1091.1(2)	1023.8(5)	978.4(3)	686.41(3)
Z	1	4	4	2	2	2
D_{calc} (g cm^{-3})	1.490	1.408	1.450	1.221	1.478	1.298
F(000)	228	416	512	404	456	292
μ(Mo Kα) (mm^{-1})	0.374	0.122	0.124	0.088	0.370	0.106
temp (K)	293	123	123	293	293	293
ω scans; *θ* range (deg)	2.32−25.0	2.28−25.0	2.35−24.99	1.67−25.0	2.31−24.99	2.32−27.49
range *h*	−1 to 5	−7 to 0	−7 to 7	−11 to 3	0 to 5	−10 to 11
range *k*	−6 to 6	0 to 10	0 to 12	−1 to 9	0 to 41	−10 to 11
range *l*	−20 to 20	−21 to 21	0 to 18	−15 to 14	−6 to 6	−12 to 12
reflns collected	2353	1884	2084	2872	1952	5599
unique reflns	2353	1612	1912	2191	1748	5599
data:parameter ratio	9.3	13.7	13.2	9.0	6.9	17.2
refinement	full-matrix least squares	full-matrix least squares	full-matrix least squares	full-matrix least squares	full-matrix least squares	full-matrix least squares
R/R^2_w (obs data)	0.0370/0.0936	0.0316/0.0858	0.0299/0.0804	0.0387/0.1119	0.0423/0.0811	0.0592/0.1140
R/R^2_w (all data)	0.0431/0.0984	0.0333/0.0872	0.0313/0.0819	0.0449/0.1252	0.0715/0.0939	0.1124/0.1377
$\Delta\rho_{max/min}$ (e Å^{-3})	0.244/−0.242	0.348/−0.273	0.204/−0.288	0.575/−0.203	0.180/−0.185	0.264/−0.215
S	1.061	1.077	1.104	1.108	1.056	1.026

malates(2−) (where hydrogen atoms have been located) revealed that no such structure had been reported. Consequently, due to the lack of structural data on organic malate(2−) salts, we have synthesized six salts, bis(4-chlorobenzyl)ammonium(1+) L-malate(2−) monohydrate (**1**), ethylenediammonium(2+) L-malate(2−) (**2**), piperazinium(2+) L-malate(2−) monohydrate (**3**), bis(3-methylbenzyl)ammonium(1+) L-malate(2−) (**4**), bis(3-chlorobenzyl)ammonium(1+) L-malate(2−) monohydrate (**5**), and 1,6-hexanediammonium(2+) L-malate monohydrate (**6**), and determined their structures using single-crystal X-ray diffraction with a view to examining packing patterns and hydrogen-bond motifs in organic malates.

Another important aspect of crystal engineering, as with most areas concerned with the solid state and structure-related properties, is the question of structural purity of a material. Due to our somewhat limited understanding of the balance between the various forces that control both crystal growth and crystal habit, the problem with structural purity (as distinct from chemical purity) is often overlooked. This is reflected by the fact that a single-crystal X-ray diffraction study (which, by definition, focuses on individual crystallites) is rarely accompanied by a powder X-ray diffraction analysis, which means that information regarding the structural purity of the whole sample is incomplete. A visual inspection of the sample may not provide conclusive information, since different polymorphs can display the same crystal habit.[10]

To examine the structural purity of **1**−**6**, powder X-ray diffraction patterns for each compound were recorded and compared with simulated patterns (from single-crystal data).

(10) Threlfall, T. L. *Analyst* **1995**, *120*, 2435.

Results

The syntheses of **1**−**6** are described in the Experimental Section, and the relevant crystallographic information is displayed in Table 1. Numbering schemes and geometries are presented in Figure 1a−f.

The X-ray single-crystal structure determinations of **1**−**6** revealed that four of the salts were hydrated, bis(4-chlorobenzyl)ammonium(1+) L-malate(2−) monohydrate, piperazinium(2+) L-malate(2−) monohydrate, bis(3-chlorobenzyl)ammonium(1+) L-malate(2−) monohydrate, and 1,6-hexanediammonium(2+) L-malate monohydrate.

The orientation of the $[-NH_3]^+$ moiety, with respect to the aromatic ring, in the six cations of **1**, **4**, and **5** displays considerable variation (−74° to 46°). This is consistent with results obtained from a search of the Cambridge Structural Database (CSD) of all organic salts containing substituted benzylammonium cations, which showed a similar distribution of N−C−C−C torsion angles. This indicates that the barrier to rotation around the exocyclic C−C bond is relatively low and may therefore be significantly influenced by intermolecular hydrogen bonds. The torsion angle N−C−C−N of the ethylenediammonium(2+) ion in **2** is ca. 77°, which is an unusual geometry, as the most common conformation for this cation is a trans configuration (less than 10% of the compounds in the CSD containing this cation deviate from such a geometry). The piperazinium(2+) cation in **3** and the 1,6-hexanediammonium cations in **6** all display the expected geometries compared with relevant data extracted from the CSD.

There is little deviation from a trans configuration in the anions of **1**−**6** (Table 2), which is analogous to the behavior displayed by hydrogen malate ions[8] and

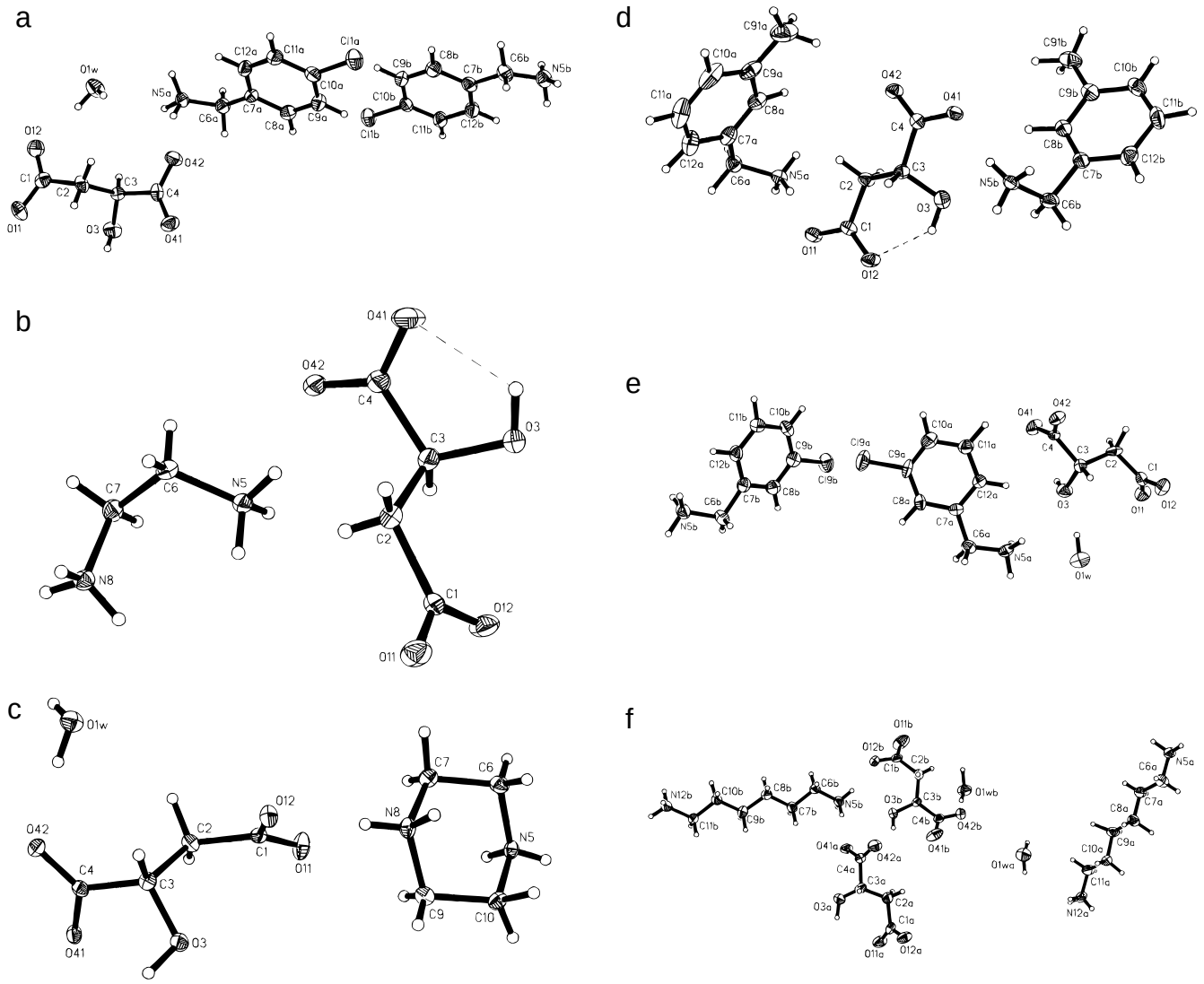

Figure 1. Geometries, thermal ellipsoids (50%) and numbering schemes of (a) **1**, (b) **2**, (c) **3**, (d) **4**, (e) **5**, and (f) **6**.

malic acid itself.[11] However, there is more variation in the O(3)−C(3)−C(4)−O(41) torsion angle (the oxygen atom of the carboxylate moiety which makes the smallest torsion angle with O(3) is consistently defined as O(41)). This is probably a reflection of the fact that the α-hydroxy group is involved in intramolecular hydrogen bonding in **2** and **4** but participates in an intermolecular hydrogen bond in **1**, **3**, **5**, and **6**. The orientation of each carboxylate moiety with respect to the anionic backbone also shows considerable variation, which is not surprising, given the diverse intermolecular hydrogen bonding taking place within these compounds.

Compound **1** with two cations, one anion, and one molecule of water has the potential for considerable hydrogen bonding with a total of seven hydrogen-bond acceptors and nine hydrogen-bond donors. There are no hydrogen-bond interactions between adjacent anions, but an infinite layer is created via a network of water−anion contacts. This layer, parallel with the *a*−*b* plane (Figure 2), contains three unique O···O interactions where each water molecule is linked to three anions. The cations are arranged in bilayers (without any unusual ring−ring distances), and the shortest Cl···Cl

Table 2. Selected Torsion Angles (deg) and Bond Lengths (Å) for 1−3

torsion angles/deg	**1**	**2**	**3**
C(1)−C(2)−C(3)−C(4)	173.42(37)	−179.71(38)	−178.54(14)
O(3)−C(3)−C(4)−O(41)	−33.86(51)	−20.13(23)	−31.31(22)
C(2)−C(3)−C(4)−O(41)	89.45(37)	101.51(19)	87.95(19)
bond lengths/Å	**1**	**2**	**3**
C(4)−O(41)	1.241(5)	1.248(2)	1.270(2)
C(4)−O(42)	1.266(5)	1.251(2)	1.248(2)
C(1)−O(11)	1.275(5)	1.253(2)	1.243(2)
C(1)−O(12)	1.256(5)	1.258(2)	1.278(2)
torsion angles/deg	**4**	**5**	**6**
C(1A)−C(2A)−C(3A)−C(4A)	−174.15(28)	174.96(83)	176.20(56)
C(1B)−C(2B)−C(3B)−C(4B)			−178.80(60)
O(3A)−C(3A)−C(4A)−O(41A)	−41.64(35)	−33.54(93)	−14.48(66)
O(3B)−C(3B)−C(4B)−O(41B)			−15.91(66)
C(2A)−C(3A)−C(4A)−O(41A)	−167.88(27)	89.75(71)	106.15(51)
C(2B)−C(3B)−C(4B)−O(41B)			107.22(47)
bond lengths/Å	**4**	**5**	**6**
C(4A)−O(41A)	1.277(4)	1.240(9)	1.244(6)
C(4A)−O(42A)	1.245(4)	1.268(9)	1.243(6)
C(4B)−O(41B)			1.235(6)
C(4B)−O(42B)			1.272(6)
C(1A)−O(11A)	1.269(4)	1.269(9)	1.239(6)
C(1A)−O(12A)	1.260(4)	1.259(9)	1.259(6)
C(1B)−O(11B)			1.227(6)
C(1B)−O(12B)			1.257(7)

(11) van der Sluis, P.; Kroon, J. *Acta Crystallogr., Sect. C* **1989**, *45*, 1406.

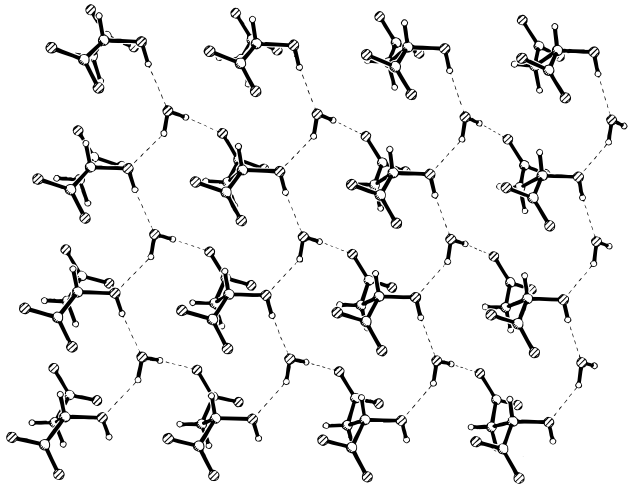

Figure 2. Anion−water layer in **1**, parallel with *a*−*b*. Hydrogen bonds indicated by dashed lines.

Table 3. Geometry of the Hydrogen Bonds in 1[a]

D−H···A	*r*(H···A)/Å	*r*(D···A)/Å	∠(D−H···A)/deg
O(3)−H(30)···O(1)′′′′′	1.966(5)	2.839(5)	174.1(1)
O(1W)−H(1W1)···O(12)	2.013(4)	2.882(4)	175.4(2)
O(1W)−H(1W2)···O(3)′′′′′′	1.985(4)	2.769(5)	145.8(1)
N(5)−H(51A)···O(41)	1.905(5)	2.814(5)	158.2(1)
N(5)−H(52A)···O(11)′	1.837(4)	2.806(4)	164.7(1)
N(5)−H(53A)···O(42)′′	1.830(5)	2.776(5)	152.5(1)
N(5)−H(51A)···O(41)′′′	1.919(5)	2.808(5)	163.6(1)
N(5)−H(52A)···O(11)′′′′	2.048(5)	2.948(5)	170.0(1)
N(5)−H(53A)···O(42)′′′′	1.846(5)	2.748(5)	142.1(2)

[a] Symmetry code: (′) $x-1, y-1, z$; (′′) $x-1, y, z$; (′′′) $x, y-1, z+1$; (′′′′) $x+1, y, z+1$; (′′′′′) $x+1, y-1, z+1$; (′′′′′′) $x+1, y+1, z$. (′′′′′′′) $x, y-1, z$.

Table 4. Geometry of the Hydrogen Bonds in 2[a]

D−H···A	*r*(H···A)/Å	*r*(D···A)/Å	∠(D−H···A)/deg
O(3)−H(3)···O(41)	2.063(2)	2.630(2)	122.54(6)
N(5)−H(51)···O(41)′	1.854(2)	2.735(2)	152.21(6)
N(5)−H(52)···O(11)′′	1.952(2)	2.702(2)	139.92(6)
N(5)−H(53)···O(42)	1.885(2)	2.737(2)	160.05(6)
N(8)−H(81)···O(12)′′′	2.135(2)	2.997(2)	167.72(6)
N(8)−H(81)···O(11)′′′	2.441(2)	3.074(2)	129.50(6)
N(8)−H(82)···O(12)′′′′	2.005(2)	2.740(2)	162.92(6)
N(8)−H(83)···O(42)′	1.901(2)	2.834(2)	169.73(6)

[a] Symmetry code: (′) $x+1, z$; (′′) $-x+2, y-1/2, -z+1/2$; (′′′) $-x+5/2, y+2, z+1/2$; (′′′′) $-x+2, y+1/2, -z+1/2$.

distance is ca. 3.81 Å. Each cation is linked to three anions via three unique H−H···O hydrogen bonds (Table 3), and there are no cation−water hydrogen bonds. The overall packing displays a 2-D nature with a water−anion layers sandwiched between cationic layers.

The ion pair of **2** contains five hydrogen-bond acceptors and seven hydrogen-bond donors, and although there are no hydrogen bonds between neighboring anions, the anions are positioned in infinite rows, parallel with *a*. In contrast to **1**, the anion contains an intramolecular hydrogen bond, *r*(O···O) 2.630(2) Å (Table 4), between the hydroxy group and its nearest carboxylate moiety. The unexpected geometry of the cation is probably induced by the good geometric "fit", involving two N−H···O hydrogen bonds, *r*[N(5)···O(41)] 2.735(2) and *r*[N(8)···O(42)] 2.834(2) Å, between one carboxylate functionality, and the $[-NH_3]^+$ moieties of each cation (Figure 3). These interactions generate nine-membered rings, incorporating both cation and anion. At the opposite end of the anion, the two

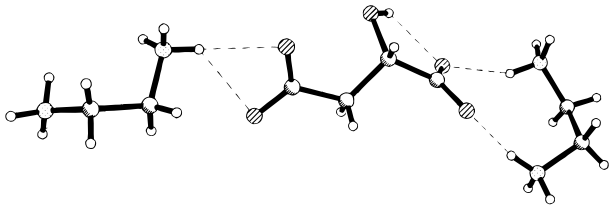

Figure 3. Hydrogen-bond interactions between cations and anion in **2**, which probably stabilize the unexpected geometry of the cation.

Table 5. Geometry of the Hydrogen Bonds in 3[a]

D−H···A	*r*(H···A)/Å	*r*(D···A)/Å	∠(D−H···A)/deg
O(1W)−H(1W1)···O(42)	1.891(2)	2.777(2)	174.85(6)
O(1W)−H(1W2)···O(3)′′′′	2.253(2)	2.938(2)	144.03(5)
O(3)−H(30)···O(11)′′′′′	1.748(2)	2.674(2)	163.07(6)
N(5)−H(51)···O(41)′	1.822(2)	2.734(2)	171.43(6)
N(5)−H(52)···O(41)′′	1.900(2)	2.715(2)	169.19(6)
N(8)−H(81)···O(12)′′′	1.828(2)	2.737(2)	143.87(6)
N(8)−H(82)···O(12)	1.925(2)	2.768(2)	174.51(6)

[a] Symmetry code: (′) $-x+1, y-1/2, -z+3/2$; (′′) $-x+3/2, -y, z-1/2$; (′′′) $x+1/2, -y+1/2, -z+1$; (′′′′) $x-1, y, z$; (′′′′′) $-x+1, y+1/2, -z+3/2$.

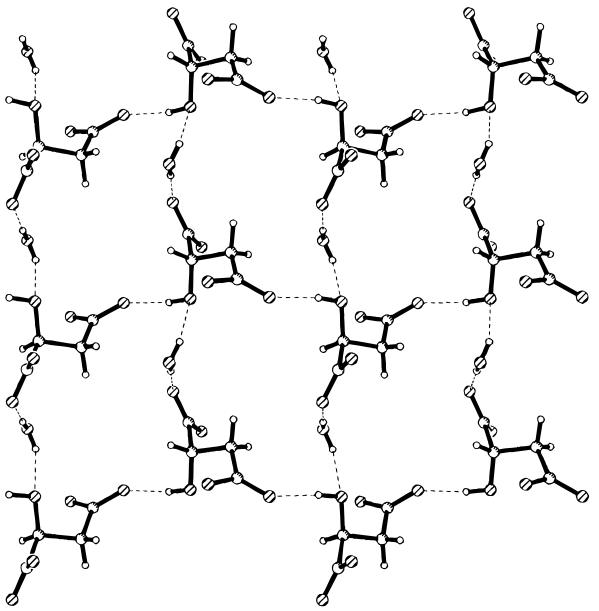

Figure 4. Infinite anion−water layer, parallel with *a*−*b*, generated by three unique hydrogen bonds in **3**.

carboxylate oxygens are involved in a bifurcated hydrogen bond, *r*[N(8)−H(81)···O(12)] 2.997(2) and *r*[N(8)−H(81)···O(11)] 3.074(2) Å. Each cation is using every available hydrogen-bond donor and is forming N···O hydrogen bonds with five anions, resulting in a highly complex 3-D network of ions, linked together by a total of seven hydrogen bonds.

In **3**, the anions do form infinite chains (parallel with *b*) via a relatively short hydrogen bond, *r*[O(3)−H(30)···O(11)] 2.674(2) Å (Table 5). Neighboring, parallel, chains are then cross-linked by water molecules, to yield an infinite 2-D architecture (parallel with *a*−*b*), generated by three O···O hydrogen bonds (Figure 4). The cations are sandwiched between anion−water layers and provide an expected "bridge", via four N···O interactions, between these layers.

The crystal structure of **4** does not, in contrast to **1** and **3**, incorporate a molecule of water in its structure. The cations are arranged in such a way as to create

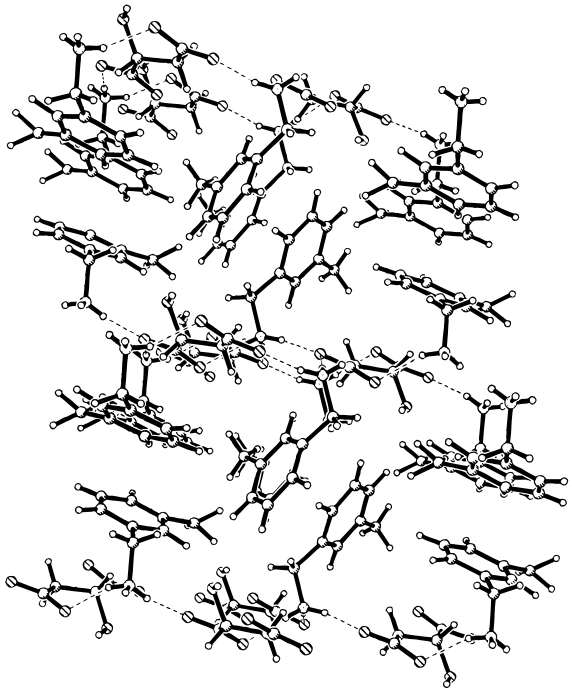

Figure 5. Layered arrangement in **4** with hydrophobic (phenyl rings) and hydrophilic (water and $[NH_3]^+$ moieties) 2-D domains.

Table 6. Geometry of the Hydrogen Bonds in 4[a]

D−H···A	*r*(H···A)/Å	*r*(D···A)/Å	∠(D−H···A)/deg
O(3)−H(30)···O(12)	1.982(3)	2.731(4)	134.8(1)
N(5A)−H(53A)···O(42)′	1.938(3)	2.748(3)	178.6(1)
N(5A)−H(52A)···O(11)	1.889(3)	2.745(3)	165.8(1)
N(5A)−H(51A)···O(11)″	1.921(4)	2.824(4)	178.5(1)
N(5B)−H(53B)···O(12)‴	2.081(3)	2.869(4)	159.57(9)
N(5B)−H(52B)···O(41)⁗	1.855(4)	2.726(4)	177.2(1)
N(5B)−H(52B)···O(41)	1.943(3)	2.773(3)	167.8(1)

[a] Symmetry code: (′) $-x+1, y+1/2, -z+1$; (″) $-x+1, y-1/2, -z+1$; (‴) $-x+1, y-1/2, -z+2$; (⁗) $-x+1, y+1/2, -z+2$.

hydrophobic (phenyl rings) and hydrophilic ($[-NH_3]^+$ moieties) 2-D domains (Figure 5). There are no face-to-face interactions between neighboring cations, but there is one short distance, *r*[C−H···C] ca. 2.62 Å, which may indicate an attractive edge-to-face interaction. Similarly to **2**, the anion does contain an intramolecular hydrogen bond, *r*[(O···O) 2.731(4) Å (Table 6). Somewhat surprisingly, this interaction takes place between the hydroxy group and the carboxylate moiety which is furthest away. Despite the absence of water, the anions are confined to a rather flat, 2-D layer, coinciding with the hydrophilic component of the cationic layer. Each cation is located at the center of three anions and is involved in an N···O hydrogen bond to each of these anions.

Although the cations of **4** and **5** are very similar, their structures show considerable differences, mainly because **5** has incorporated one molecule of water into its lattice. As a consequence, a water−anion layer is generated via three unique hydrogen bonds (Figure 6), similar to the anion−water layer in **1**. There are no anion−anion hydrogen bonds, and each water molecule is linked to three anions (Table 7). There are no hydrogen bonds between anions and cations, and the water−anion layer is sandwiched between layers of cations.

The crystal structure of **6** contains ribbons of alternating anions and water molecules, held together by a

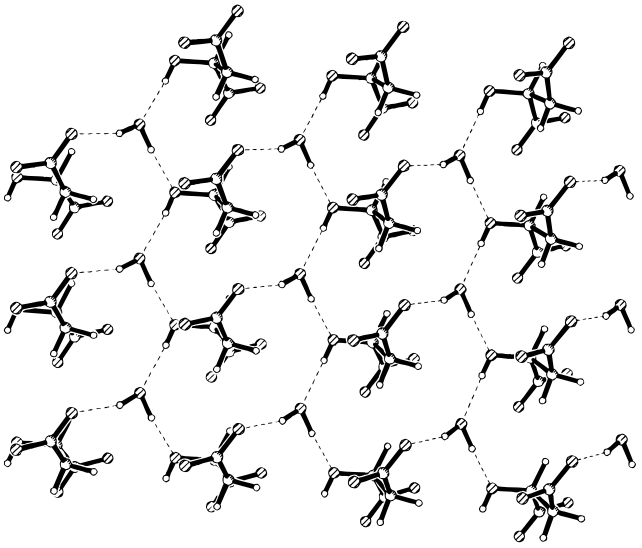

Figure 6. Anion−water layer in **5**, generated by three unique O···O hydrogen bonds.

Table 7. Geometry of the Hydrogen Bonds in 5[a]

D−H···A	*r*(H···A)/Å	*r*(D···A)/Å	∠(D−H···A)/deg
O(1W)−H(1W1)···O(3)	1.810(8)	2.783(9)	166.87(27)
O(1W)−H(1W2)···O(12)″	1.972(9)	2.878(9)	160.72(30)
O(3)−H(30)···O(1W)‴‴‴	2.051(9)	2.827(9)	156.73(23)
N(5A)−H(51A)···O(42)′	1.826(9)	2.779(9)	172.05(27)
N(5A)−H(52A)···O(42)″	1.986(9)	2.816(9)	149.60(22)
N(5A)−H(53A)···O(41)‴	1.754(8)	2.787(8)	169.54(27)
N(5B)−H(51B)···O(11)⁗	1.786(10)	2.754(1)	159.14(28)
N(5B)−H(52B)···O(12)⁗⁗	1.960(9)	2.973(9)	167.00(26)
N(5B)−H(53B)···O(11)⁗⁗	1.899(10)	2.804(10)	158.88(27)

[a] Symmetry code: (′) $x+1, y, z-1$; (″) $x, y, z-1$; (‴) $x+1, y, z$; (⁗) $-x+1, y-1/2, -z$. (⁗⁗) $-x+1, y-1/2, -z+1$; (⁗⁗⁗) $-x, y-1/2, -z$; (⁗⁗⁗⁗) $x-1, y, z$.

Table 8. Geometry of the Hydrogen Bonds in 6[a]

D−H···A	*r*(H···A)/Å	*r*(D···A)/Å	∠(D−H···A)/deg
O(3A)−H(30A)···O(11B)[j]	1.925(5)	2.810(5)	153.78(15)
O(3B)−H(30B)···O(42B)	2.164(5)	2.617(5)	103.89(14)
O(3B)−H(30B)···O(41A)	2.239(5)	3.175(5)	148.87(12)
O(1WA)−H(1WA)···O(12B)[d]	1.946(6)	2.932(6)	160.39(16)
O(1WA)−H(2WA)···O(41A)[d]	1.894(5)	2.842(5)	173.11(17)
O(1WB)−H(1WB)···O(41B)	1.777(6)	2.841(6)	168.10(16)
O(1WB)−H(2WB)···O(11A)[k]	1.562(5)	2.697(5)	168.54(21)
N(5A)−H(51A)···O(41B)[a]	2.132(6)	2.961(6)	140.58(17)
N(5A)−H(51A)···O(42B)[a]	2.381(6)	3.287(6)	152.34(13)
N(5A)−H(52A)···O(1WA)[a]	2.050(6)	2.796(6)	139.40(17)
N(5A)−H(53A)···O(11A)[b]	2.217(6)	2.906(6)	137.51(17)
N(5B)−H(51B)···O(12A)[c]	1.877(5)	2.804(5)	158.42(17)
N(5B)−H(52B)···O(42A)	1.963(5)	2.782(5)	174.89(15)
N(5B)−H(53B)···O(12B)	2.009(5)	2.849(5)	157.57(18)
N(12A)−H(12A)···O(41A)[d]	2.153(5)	2.943(5)	147.66(17)
N(12A)−H(12B)···O(12B)[e]	2.084(6)	2.902(6)	172.38(18)
N(12A)−H(12C)···O(O1WB)[f]	1.764(6)	2.827(6)	170.97(18)
N(12B)−H(12D)···O(41B)[g]	1.908(5)	2.746(5)	149.27(18)
N(12B)−H(12E)···O(12A)[h]	1.881(5)	2.759(5)	174.28(18)
N(12B)−H(12F)···O(42A)[i]	2.011(6)	2.796(6)	153.60(15)

[a] Symmetry code: $x, y, z+1$; [b] $x, y, z+2$; [c] $x-1, y, z$; [d] $x, y+1, z$; [e] $x+1, y+1, z$; [f] $x+1, y, z$; [g] $x, y-1, z-1$; [h] $x-1, y-1, z$; [i] $x, y-1$; [j] $x+1, y, z-1$; [k] $x-1, y, z+1$.

total of six hydrogen bonds (Table 8, Figure 7). The cations provide a "bridge" between neighboring anion−water ribbons, to create an intricate 3-D hydrogen-bonded network. The cation is also involved in a bifurcated hydrogen bond, *r*[N(5a)−H(51A)···O(42B)] 2.961(6) and *r*[N(5A)−H(51A)···O(41B)] 3.287(6) Å.

Finally, to verify that the chosen single crystals were representative of the bulk materials, the X-ray powder diffraction patterns were simulated from the single-

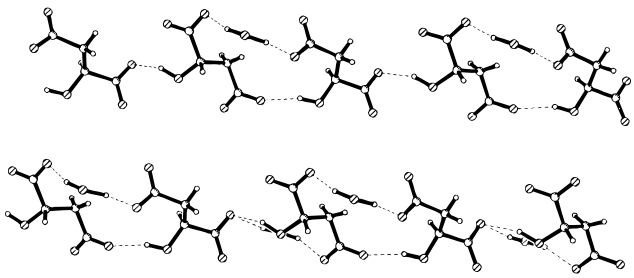

Figure 7. Arrangement of water molecules and malate(2−) anions in **6**, forming infinite, hydrogen-bonded ribbons.

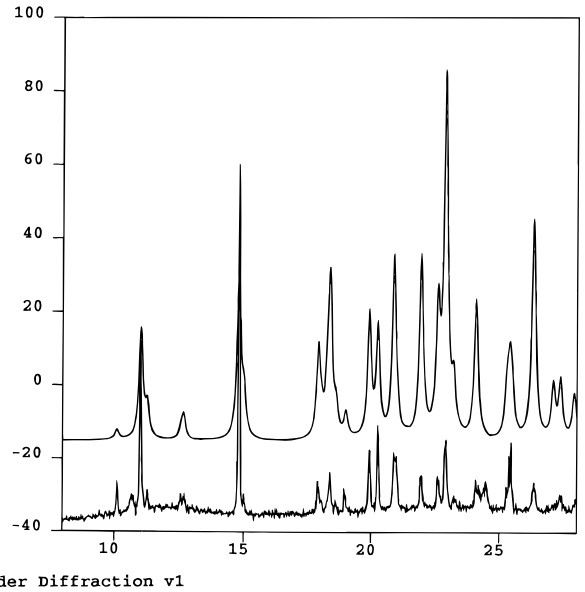

Figure 8. Comparison of the experimental powder X-ray diffraction pattern (bottom) with the simulated powder X-ray diffraction pattern (top) from the single-crystal data of **6**.

crystal data (using Cerius[2]) and compared with the experimental X-ray powder patterns, recorded on bulk samples of **1**−**6**. The match between simulated and experimental pattern demonstrated that only one structural form of **1**−**6** was present in each case. The relevant patterns for **6** are shown in Figure 8. Although the intensities (which are sensitive to crystallite shape and preferred orientation) are considerably different, peak positions indicative of the lattice parameters are very similar for experimental and calculated patterns.

Discussion

An examination of six crystal structures containing the L-malate(2−) anion has demonstrated that this anion participates in a wide variety of structural motifs, in contrast to the structurally reliable hydrogen malate ion. Having eliminated the possibility of a head-to-tail hydrogen bond between neighboring anions in organic malate(2−) salts, the basis for a 2-D hydrogen-bonded anionic motif is removed, and as a consequence there are no recognizable, reoccurring anionic aggregates within this series of compounds. Four of the six structures have also incorporated water molecules in the lattice, whereas the vast majority of extant organic hydrogen malates are nonhydrated.[12] It may be argued that different results would be obtained if the compounds were prepared under strict anhydrous conditions, but this does not detract from the fact that the two families of compounds behave very differently toward water. The question of when, or if, water is going to be incorporated into the solid-state structure is clearly an important and highly complicated issue, which has been addressed in depth by Jeffrey and Saenger.[13] At this point in time, the presence of water molecules in **1**, **3**, **5**, and **6**, but not in **2** and **4**, is somewhat difficult to explain. However, in **1**, **3**, and **5**, the water molecule acts as a cross-link between anions, hence providing a substitute for the "missing" hydrogen-bond donor (compared to the hydrogen malate anion). In these cases, there are also no intramolecular hydrogen bonds within the anions, whereas when water is absent (**2** and **4**), the malate(2−) anion contains an intramolecular hydrogen bond. Further work is needed to establish possible correlations between the presence of water and the specific properties of the cation.[14]

By comparing structures of hydrogen malates and malates, it is clear that the presence, or absence, of even a single, strong, hydrogen-bond interaction makes a crucial difference to the 3-D structural aggregation of ions in the solid state. The strength and selectivity of the head-to-tail O−H···O interaction in hydrogen malate salts, even in the presence of other electrostatic forces, provides a secure basis for the construction of reoccurring 2-D anionic architectures. Since there are no strong, directional forces between anions in the malate salts, weaker hydrogen bonds and other intermolecular interactions accept a larger responsibility for determining the final arrangement of the building blocks in these compounds.

Although we have only mentioned the influence of relatively strong hydrogen bonds, e.g., N−H···O and O−H···O, on the structures of **1**−**6**, we also explored the possibilities for weaker intermolecular interactions by searching for unexpected, or unusual, C−H···O geometries. However, such interactions did not seem to play a significant part in determining the assembly of ionic building blocks in **1**−**6**. This assessment was based upon conventional geometric search criteria, but, in addition, there were no obvious patterns or motifs involving C−H···O in this series of compounds. The seeming lack of influence of weaker hydrogen bonds is not too surprising, since there is a multitude of much stronger hydrogen bonds present in each case which would seem to dominate the assembly process.

The flexibility of the anion is demonstrated by the fact that the torsion angles of the anions display a variety of values indicative of low torsional barriers. The only consistent value is obtained for the torsion involving the C−C−C−C backbone which, consistently, exhibits a value close to 180°. A similar behavior has been noted in the geometry of the hydrogen malate anion; flexibility in most torsion angles apart from the backbone of the ion.

The comparison of experimental X-ray powder diffraction data with powder data generated from the relevant crystal structures (as determined by single-crystal techniques) demonstrated that the bulk mate-

(12) Aakeröy, C. B.; Nieuwenhuyzen, M., unpublished results.

(13) Jeffrey, G. A.; Saenger, W. *Hydrogen Bonding in Biological Structures*; Springer: Berlin, 1991.

(14) We are in the process of examining this issue specifically in the context of hydrogen malates/malates and hydrogen tartrates/tartrates, but those results will be presented at a later date.

rial, in all six cases, was structurally homogeneous, and corresponded to the single-crystal structure. Despite discrepancies in intensities (due to a certain degree of preferred orientations of the powdered samples), there were no significant spurious peaks in the experimental data sets.

Conclusions

The directionality and selectivity of the hydrogen bond has been widely employed in crystal engineering strategies of multidimensional, predictable motifs. The anion in most organic hydrogen malate salts creates a distinctive 2-D motif, irrespective of the characteristics of the cation. Malate(2−) anions, however, assemble in a variety of structural patterns, viz., chains, layers, and ribbons, without a preference for a specific motif. Thus, this study has emphasized that the balance between intermolecular and electrostatic forces can be substantially altered by the suitable choice (addition or removal) of a strong hydrogen-bond interaction. This provides additional support to the notion that the hydrogen bond can be used as a tool in intermolecular design of predictable ionic architectures which, in turn, can be used as scaffolding for new optical, electrical, or magnetic materials.

Finally, given the importance of a complete structural analysis of bulk materials (not just of individual crystals) for understanding, and rationalizing structure-property correlations in the solid state, it seems that a combination of X-ray single-crystal and powder diffraction techniques, as described herein, should be adopted as a matter of routine (where possible) in all areas of crystal engineering and crystal structure determinations.

Experimental Section

Preparation of Bis(4-chlorobenzyl)ammonium(1+) *L*-Malate(2−) Monohydrate (1). An enthanolic solution (10 cm^3) of 4-chlorobenzylamine (6.1 mmol) was mixed with an aqueous solution (10 cm^3) of *L*-malic acid (3.1 mmol). A white solid appeared after slow evaporation of the solvents. The product was collected by filtration and recrystallized from water to produce clear, colorless crystals. Found: C, 49.3; H, 5.3; N, 6.4%. Calculated for $C_{18}H_{24}Cl_2N_2O_6$: C, 49.67; H, 5.56; N, 6.44%. Mp 171−173 °C.

Preparation of Ethylenediammonium(2+) *L*-Malate-(2−) (2). An ethanolic solution (10 cm^3) of ethylenediamine (3.3 mmol) was mixed with an aqueous solution (10 cm^3) of *L*-malic acid (3.1 mmol). The mixture was heated gently for 5 min. A white solid appeared after evaporation of the solvents. The product was collected recrystallized from EtOH/H_2O (50:50) to yield colorless crystals. Found: C, 49.4: H, 6.1; N, 11.4%. Calculated for $C_6H_{14}N_2O_5$: C, 49.58; H, 5.83; N, 11.56%. Mp 98−99 °C.

Preparation of Piperazinium(2+) *L*-Malate(2−) Monohydrate (3). An aqueous solution (20 cm^3) of piperazine (3.3 mmol) was mixed with an aqueous solution (15 cm^3) of *L*-malic acid (3.1 mmol). The solvent was evaporated by warming on hot plate until a white precipitate formed. The product was collected by filtration and recrystallized from water to produce clear, colorless crystals. Found: C, 40.5; H, 7.5; N, 11.3%. Calculated for $C_8H_{18}N_2O_5$: C, 40.33; H, 7.62; N, 11.76%. Mp 219−221 °C.

Preparation of Bis(3-methylbenzyl)ammonium(1+) *L*-Malate(2−) (4). An ethanolic solution (10 cm^3) of 3-methylbenzylamine (6.0 mmol) was mixed with an aqueous solution (10 cm^3) of *L*-malic acid (3.0 mmol). The solvent was allowed to evaporate at ambient temperatures until a white precipitate formed. The product was recrystallized from water to produce clear, colorless crystals. Found: C, 63.1; H, 7.4; N, 7.0%. Calculated for $C_{20}H_{28}N_2O_5$: C, 63.81; H, 7.50; N, 7.44%. Mp 124−127 °C.

Preparation of Bis(3-chlorobenzyl)ammonium(1+) *L*-Malate(2−) Monohydrate (5). An aqueous solution (10 cm^3) of 3-chlorobenzylamine (6.1 mmol) was mixed with an aqueous solution (10 cm^3) of *L*-malic acid (3.0 mmol). The solvent was slowly evaporated at ambient temperatures until a white precipitate formed. The product was collected by filtration and recrystallized from water to produce colorless crystals. Found: C, 50.1; H, 5.5; N, 6.0%. Calculated for $C_{20}H_{28}N_2O_5$: C, 49.67; H, 5.56; N, 6.44%. Mp 109−111 °C.

Preparation of 1,6-Hexanediammonium(2+) *L*-Malate-(2−) Monohydrate (6). An ethanolic solution (10 cm^3) of 1,6-hexanediamine (3.1 mmol) was mixed with an aqueous solution (10 cm^3) of *L*-malic acid (3.1). The mixture was heated, while stirring, for 10 min. The solvent was then slowly evaporated until a white precipitate formed. The product was collected by filtration and recrystallized from water/ethanol (50:50) to produce clear, colorless crystals. Found: C, 45.1; H, 9.1; N, 10.5%. Calculated for $C_{10}H_{26}N_2O_7$: C, 44.77; H, 9.02; N, 10.44%. Mp 99−101 °C.

X-ray Crystallography: Single-Crystal Data. Crystal data were collected using a Siemens P4 four-circle diffractometer with graphite monochromated Mo Kα radiation. Crystal stabilities were monitored by measuring standard reflections every 100 reflections, and there were no significant variations (<±1%). Cell parameters were obtained from 35 accurately centered reflections in the 2θ range 10−28°. ω scans were employed for data collection, and Lorentz and polarization corrections were applied. The configuration for the salts was determined by the fact that enantiomerically pure *L*-malic acid was used as starting material for all products.

The structures were solved by direct methods, and the non-hydrogen atoms were refined with anisotropic thermal prameters. Hydrogen-atom positions were located from difference Fourier maps, and a riding model with fixed thermal parameters ($U_{ij} = 1.5U_{ij}$(eq) for the atom to which they are bonded) was used for subsequent refinements. The function minimized was $\sum[\omega(|F_o|^2 - |F_c|^2)]$ with reflection weights $\omega^{-1} = [\sigma^2|F_o|^2 + (g_1P)^2 + (g_2P)]$, where $P = [\max|F_o|^2 + 2|F_c|^2]/3$. The SHELXTL PC and SHELXL-93 packages were used for data reduction and structure solution and refinement.[15]

X-ray Crystallography: Powder Data. Data were recorded on a Siemens D5000 in reflectance geometry with a step size of 0.01 2θ and a scan time of 0.2 s over the 2θ range 5−40. Each sample was carefully ground in order to avoid detrimental effects due to preferential crystal growth. Simulated powder patterns, based upon single-crystal data, were obtained with the *Diffraction* module in Cerius[2].

Supporting Information Available: Tables of atomic coordinates, isotropic and anisotropic displacement coefficients, and bond lengths and angles (33 pages); structure factor tables (37 pages). Ordering information is given on any current masthead page.

Acknowledgment. Financial support from DRA (Fort Halstead) and the NIDevR is gratefully acknowledged.

CM950524B

(15) Sheldrick, G. M. SHELXL-93, University of Göttingen.